

Statistical characterisation of bio-aerosol background in an urban environment

M. Jamriska*, T.C. DuBois, A. Skvortsov

Defence Science and Technology Organisation, 506 Lorimer Street, Fishermans Bend, Victoria 3207, Australia

ARTICLE INFO

Article history:

Received 27 October 2011

Received in revised form

8 February 2012

Accepted 13 February 2012

Keywords:

Aerosol
Biobackground
Biodetection
Model
Algorithm
Turbulent mixing

PACS:

47.27.nb

47.27.eb

05.45.Tp

92.60.Fm

92.60.Mt

ABSTRACT

In this paper we statistically characterise the bio-aerosol background in an urban environment. To do this we measure concentration levels of naturally occurring microbiological material in the atmosphere over several days. Naturally occurring bio-aerosols can be considered as noise, as they mask the presence of signals coming from biological material of interest (such as an intentionally released biological agent). Analysis of this ‘biobackground’ was undertaken in the 1–10 μm size range and a 3–9% contribution was found to be biological in origin – values which are in good agreement with other studies reported in the literature. A model based on the physics of turbulent mixing and dispersion was developed and validated against this analysis. The Gamma distribution (the basis of our model) is shown to comply with the scaling laws of the concentration moments of our data, which enables us to universally characterise both biological and non-biological material in the atmosphere. An application of this model is proposed to build a framework for the development of novel algorithms for bio-aerosol detection and rapid characterisation.

Crown Copyright © 2012 Published by Elsevier Ltd. All rights reserved.

1. Introduction

It is well recognised that biogenic aerosols have a significant effect on human health, the environment, climate, atmosphere and other phenomena (Pöschl, 2005; Jaenicke et al., 2007; Ho and Duncan, 2005; Huffman et al., 2010 and references therein). Numerous studies have been conducted that focus on the characterisation of naturally occurring microbiological material in the atmosphere (referred in this paper as biobackground) (Bauer et al., 2008). This large body of literature indicates a rich and diversified dependence of biobackground characteristics affected by geographical location, temporal, seasonal and daily variations as well as the dependency on applied measuring techniques (Ho and Spence, 1998). A comprehensive review of publications concerning bio-aerosol studies is outside of the scope of the current paper and the readers are referred to a number of recently published reviews (Huffman et al., 2010; Burrows et al., 2009; Harrison et al., 2004; Jaenicke et al., 2007; Ariya et al., 2009 and references therein).

Biobackground is the primary limiting factor of biodetection technologies used in operational applications (bio-security, defence systems and counterterrorism) (Ho and Duncan, 2005; Jensen, 2007). As discussed below, this limitation is associated with the less than “optimal” selectivity and specificity of the current available biodetectors.

Naturally occurring bio-aerosols can be considered as noise, as they mask the presence of signals coming from biological material of interest (e.g. an intentionally released biological agent), hindering a biodetectors’ capability (by affecting its sensitivity, selectivity, time of response or rate of false alarms) to detect airborne biological threats.¹

Selection of a specific technique for bio-aerosol detection is a challenging task, whose outcome is determined by both the intended application and the scenario in which it is deployed (Buteau et al., 2010). It is unlikely that a single biodetection technique capable of detecting all biological agents will be developed in the foreseeable future. This necessitates the use of multiple, often complementary technologies and data processing algorithms for

* Corresponding author.

E-mail addresses: milan.jamriska@dsto.defence.gov.au, ljamriska@bigpond.au (M. Jamriska).

¹ A review of biodetection methods and technologies is presented for example in TRW Systems and Information Technology Group (2001).

reliable bio-threat detection. The consistent integration of these technologies into a single operational system is influenced by the critical issue of 'data fusion' of multiple information sources, i.e. the rigorous comparison of the relative information gain that can be provided by a particular biodetection technique. Apparently this issue cannot be thoroughly investigated and eliminated without detailed knowledge of the biobackground the proposed system is operational in. From this perspective; understanding the characteristics, dependencies and parameters affecting the biobackground is a critical step in the development of enhanced biodetection capability operating over a broad spectrum of applications and scenarios. More specifically, development of an accurate model of biobackground, as presented in this study, will assist in the definition of an optimal sampling protocol (sampling rate and volume) in order to detect a given biological threat. This in turn will determine the optimal performance of the proposed biodetection system and will provide a consistent way of evaluating various sensor and detection technologies (which are capable of implementing such a protocol) and establish the theoretical limits for improvement of the existing systems.

Particles in the ambient environment (atmospheric surface layer) are in continuous chaotic motion being advected by turbulent flow. Since most of these particles are very small (less than 10 μm) their inverse effect on flow is negligible and their kinematics can be described by the models of 'passive scalars' (i.e. a system of passive markers associated with the individual particles randomly moving by turbulence) (Falkovich et al., 2001). Under this condition it is reasonable to assume that the fundamental physical properties of turbulent mixing and not the physical properties of the particles (e.g. size, density etc.) would strongly emerge in the statistical characteristics of the biobackground. These characteristics are determined by the kinematics of the turbulent flow and are therefore independent of the origin or nature of the particles (i.e. biological or non-biological).

An illustrative example of this approach has been recently reported in our publication, Skvortsov et al. (2010), where we established scaling laws of time series for particle concentration and found they comply with specific models of turbulent mixing (Yee and Chan, 1997; Villiermaux and Duplat, 2003). These results provide the motivation and foundation for the current study, i.e. the application of the theoretical methods of passive tracer dispersion in the atmospheric surface layer to deduce the universal statistics (scaling laws) of particles regardless of their origin.

The current study focuses on a biodetection framework which enables a consistent prediction of some of the statistical properties of particle concentrations in the biobackground (moments, probability distribution functions (PDFs), intermittency corrections, etc.) by employing well-known properties of turbulent mixing (Yee and Chan, 1997; Villiermaux and Duplat, 2003; Lebedev and Turitsyn, 2004; Yee, 2009; Skvortsov and Yee, 2011).

The main rationale behind the proposed framework is to integrate a pure statistical approach to bio-aerosol background characterisation (when statistical properties of concentration time-series are simply postulated) using the physical properties of turbulent mixing. The integrated model should be able to assist in finding key associations between the statistical characteristics of the bio-aerosol background in terms of the universal (physical) parameters of atmospheric turbulence and cater for their variation. The statistical framework presented was validated using a large data set of biological and non-biological particle concentrations measured by an optical biodetector utilising laser induced auto-fluorescence characteristics for living organisms (Hairston et al., 1997; Ho and Spence, 1998; Brosseau et al., 2000). We also discuss the applicability of this statistical approach for the development of detection algorithms in operational systems.

The framework was developed in two steps: first, we collected a large data set of physical characteristics of the ambient biobackground. The data were screened, validated, analysed and results compared to literature. This provided the quantification of a validated biobackground data set for an urban/industrial type of ambient environment. We then developed a mathematical model based on statistical properties (such as moments) derived from analysis of time series of measured data, revealing analytical forms of concentration PDFs characteristic of the ambient biobackground. The derived generic PDFs (Probability Distribution Functions) are fundamental to the development of the next generation of biodetection algorithms.

The paper is organized as follows: in the first part we outline the measuring methodology and present quantification results of the biobackground; in the second part we present the statistical model, its validation and the analytical PDF forms derived from our measured data.

2. Experimental

2.1. Instrumentation

The atmospheric aerosol was measured and characterised by two instruments: Fluorescent Aerosol Particle System (FLAPS-III, Dycor Technologies) and Aerodynamic Particle Sizer (APS, TSI Model 3321). Both have been used in a variety of aerosol research studies including the areas of environmental and biobackground monitoring (Huffman et al., 2010 and references therein), hence only a brief description follows.

FLAPS-III is an integrated optical biodetection system providing near real time (few seconds) point-detection of particles of biological origin (Dycor, 2011a). It utilises laser induced auto-fluorescence intrinsic to living biological organisms (Boulet et al., 1996; Hairston et al., 1997; Hill et al., 1999; Ho and Spence, 1998; Eng et al., 1989; Setlow and Setlow, 1977; Laflamme et al., 2005; Agranovski and Ristovski, 2005; Huffman et al., 2010). The system is comprised of two major components: FLAPS-III (TSI Model 3317) and particle concentrator (XMX/2A, Dycor Technologies). FLAPS-III measures side scattering (SS) and fluorescence (FL) light intensities of a single particle. The fluorescence signal is measured in two wavelength bands corresponding to the emissions from NAD(P)H (FL1) and riboflavin (FL2) (Hairston et al., 1997; Boulet et al., 1996; Hill et al., 1999). In conjunction with the XMX concentrator the system provides count rates of total (TAP) and fluorescent biological aerosol particles (FBAPs) in the 1–10 μm size range. The system (XMX/2A concentrator, FLAPS, software) was developed primarily as a biodetection unit with a limited capability for an accurate quantification of particle concentration in the sampled ambient air. The detector does not allow identification or speciation of the detected bio-particles (Dycor, 2011b). Detailed descriptions of the instrument and operating principles are presented elsewhere (Hairston et al., 1997; Pinnick et al., 1998; Agranovski et al., 2003b).

FLAPS-III is currently considered as one of the benchmark biodetectors for use in defence applications. The system has been evaluated for accuracy, sensitivity and reliability in numerous laboratory and field studies using biological agents and simulants and has proved to be a reliable and accurate biodetector (Ho and Spence, 1998; Ho et al., 1999; Semler et al., 2004; Agranovski and Ristovski, 2005). Huffman et al. (2010) demonstrated the suitability of FLAPS-III for field studies and biobackground characterisation.

APS is a time-of-flight optical spectrometer measuring number concentration and size characteristics of particles in the 0.5–20 μm size range. For the purposes of this study the APS measurement data was truncated to the 1–10 μm size range to match data

measured by FLAPS-III. Assuming particle sphericity and known density; *surface, volume* and *mass* characteristics of particles can be estimated from the measured data. More detail about the APS instrument is presented in Baron and Willeke (2005); TSI (2011); Peters and Leith (2003); Tsai et al. (2004).

2.2. Instruments settings and calibration

APS and FLAPS-III were factory calibrated prior the commencement of the study and maintained during the measuring campaign according to their respective manuals. The operational settings for FLAPS-III recommended by the manufacturer were experimentally validated using aerosol challenges of known characteristics (Kanaani et al., 2008; Agranovski et al., 2004; Huffman et al., 2010).

The SS and FL signals measured by FLAPS-III are each gated into overall 32 bins according to the increasing SS and FL light intensities. Based on experimental results which were in agreement with the manufacturer's recommendation, bins [2–31] (where bin 0 is the first bin) were selected for the measurement of fluorescent (FL1 and FL2) signals, and bins [0–31] for the measurement of SS signals. Settings for LED power and PMT gain were determined using non-fluorescent PSL spheres and NaCl aerosols following the method outlined in Brosseau et al., 2000. FLAPS-III operated in a continuous sampling mode with the concentrator flowrate set at maximum (350 L min^{-1}) and aerosol stream flowrate 1 L min^{-1} .

2.3. Fluorescent biological aerosol particles

Fluorescent biological aerosol particles (FBAPs) measured by FLAPS-III represent a subset of primary biological aerosol particles (PBAPs). PBAP can be defined as a particle that discernibly is or was all or part of a living organism (Gabey et al., 2009; Pinnick et al., 2009; Huffman et al., 2010). Ho and Spence (1998) demonstrated that the FBAPs measured by FLAPS-III technology are attributed mainly to the presence of biological material. The measured count of FBAPs may be considered as a conservative estimate of the PBAPs' abundance in the ambient air (Huffman et al., 2010).

Some particles, despite being of non-biological origin, also exhibit fluorescence (Agranovski et al., 2003a; Sivaprakasam et al., 2004), however the contribution of these interferents to the overall FL counts measured by FLAPS-III for most ambient conditions and the size range of interest ($1\text{--}10 \mu\text{m}$) can be neglected (Pinnick et al., 2009; Ho et al., 1999 and references therein).

Since FLAPS-III does not provide direct quantification of aerosol concentration – only an integrated count of particles detected in the sampled volume is available – it was used in parallel with the APS. The concentration of FBAP was then estimated from the total particle concentration measured by APS and the fraction of fluorescent particles in the total count was determined from FLAPS-III data (FL/SS ratio).

3. Methods

3.1. Air sampling

The measurements were conducted on the top of a four story building at 12 m height with the instrumentation housed inside an air-conditioned environmental enclosure. The ambient air was sampled through vertical conductive sampling lines protruding about 1.5 m outside of the enclosure's ceiling.

Deposition losses of particles in sampling lines were assessed experimentally and theoretically (Baron and Willeke, 2005) and found to be negligible (less than 2%). Sampling was done on a semi-continuous basis with the interruptions due to instrument

maintenance and availability. Both APS and FLAPS-III operated side by side and provided measurements every 5 s.

3.2. Measurement location

The sampling site was located near Port Melbourne ($-37^{\circ}49'27.45''$, $+144^{\circ}54'43.02''$), approximately 0.5 km South from the Yarra River; 5 km West from the Melbourne CBD and 3 km North of Port Philip Bay. The site is representative of an urban/industrial environment influenced by marine sources during SE to SW wind conditions. The dominant local sources contributing to the ambient background are attributed to the emissions from several manufacturing factories (car industry; business parks; dockside) in the area and vehicular traffic emissions originating from two major freeways surrounding the monitoring site from East to West (in a semicircle) and to a lesser degree local traffic on nearby roads. The freeways are located about 1–2 km away from the sampling site and carry, in general, high traffic volume throughout the day with the traffic peak hours between 07:00–10:00 and 16:00–20:00. In terms of local biogenic sources; there is a park area about 1 km SSW from the sampling site. The topography in the area is open and flat.

3.3. Meteorological conditions

Representative meteorological data have been obtained from three meteorological stations (Bureau of Meteorology sites) located 5–13 km North, SW and SE from the sampling site. The air temperature and RH were in the ranges of $1\text{--}23^{\circ} \text{C}$ & $36\text{--}100\%$ with mean values of 11°C and 80%, respectively. Rainfall for the period was approximately 37 mm per month, with an average of 12.5 rainy days per month. The prevalent wind conditions for the duration of the measuring campaign were WSW with average wind speeds of $2\text{--}4 \text{ m s}^{-1}$.

3.4. Data collection and processing

Data were collected over 28 days between 27/04/2009 and 23/06/2009. Approximately 500 h and 340 h of data (5 s readings) were measured by FLAPS-III and APS, respectively. About 140 h of data were measured simultaneously by both instruments. The data obtained were screened for outliers and anomalies, processed and stored in a custom built SQL database. A set of programming tools allowing data manipulation, retrieval and averaging was developed using MATLAB. Exploratory and statistical analysis was performed using MATLAB and S-Plus software packages.

4. Data inspection

Before discussing our turbulent mixing and dispersion model, it is important to investigate some of the properties of the experimental measurements acquired throughout the campaign and validate the data set against similar studies. Simple statistics for APS and FLAPS-III data are presented in Tables 1 and 2, respectively.

4.1. APS data

The median values of particle *number* concentration (dN) and *mass* concentration (dM) in the $1\text{--}10 \mu\text{m}$ size range measured by APS were $1.5 \# \text{ cm}^{-3}$ and 0.006 mg m^{-3} , respectively. Median values are presented throughout this paper as a better estimate (compared to mean) due to skewed distribution of measured data distribution (Ho and Spence, 1998; Morawska et al., 1999).

A relatively low *number* concentration of particles is expected, as the majority of particles in an urban/industrial type of

Table 1

Statistics for aerosol data measured by APS ($n \sim 245,374$; total sampling time ~ 340 h). Particle mass concentration dM was estimated from volume concentration dV and a particle density of $\approx 1 \text{ g cm}^{-3}$. dN and dM denote particle number and mass concentration; CMD denotes particles count median diameter.

Parameter measured	Mean	STD	Median	IQR
Conc dN [1–10 μm] ($\# \text{ cm}^{-3}$)	2.189	1.970	1.500	0.840
CMD dN [1–10 μm] (μm)	1.500	0.101	1.486	0.107
Conc dM [1–10 μm] (mg m^{-3})	0.009	0.007	0.006	0.004
CMD dM [1–10 μm] (μm)	3.122	1.115	2.839	0.533

environment is dominated by combustion sources (e.g. traffic emissions); generating predominantly fine, submicrometer particles (Jamriska et al., 2008; Mejía et al., 2007) which are outside of the size range considered in this study.

Particle mass concentration in the 1–10 μm size range (dM [1–10 μm]) derived from APS number data is also relatively low, reflecting the dominance of fine particles. An indirect comparison of the measured dM results with literature data indicates a good agreement. Keywood et al. (1999) characterised PM concentrations in six Australian cities, reporting a mean value of PM/PM ratio of 0.45; i.e. approximately 55% of PM mass concentration is attributed to particles in the 1–10 μm size range. Using this estimate and an ambient particle density of 1.6 g cm^{-3} (Morawska et al., 1999; Pitz et al., 2003) the estimates for the PM derived from our data are 0.026 mg m^{-3} (mean) and 0.017 mg m^{-3} (median). These results are in good agreement with the annual mean PM value for Melbourne of $0.023 \pm 0.009 \text{ mg m}^{-3}$ reported by Keywood et al. (1999) as well as EPA data reported for the monitoring time period ($0.020\text{--}0.024 \text{ mg m}^{-3}$) (Environmental Protection Agency, 2009).

In terms of particle size distribution, the corresponding median diameter for particle number and mass distribution was $1.5 \mu\text{m}$ and $2.8 \mu\text{m}$, respectively. The results presented are based on the analysis of the available data for particles in the 1–10 μm size range. While there is limited information or data on the size distribution statistics of this particular size range, our results are in a relatively good agreement with findings reported by Huffman et al. (2010).

In order to discern emission sources dominating the ambient background during different time periods, the results were grouped into three time intervals: day (06:00–20:00), night (20:00–06:00) and 24 h (00:00–24:00) measurements. The statistics for these groups in the form of boxplots is presented in Fig. 1.

Visual observation of the data presented indicates that the mean and median values for the day, night and 24 h data sets are comparable for both particle number and particle mass concentration, however statistical analysis of the medians difference (Mann–Whitney two sample rank-sum test) reveals a significant difference between the medians of all three groups (at the 95% confidence level). There seems to be less fluctuation (i.e. spread of the data as indicated by IQR) in day data as compared to night data. This is likely associated with traffic emissions dominating the ambient background during day time (06:00–20:00) (Mejía et al., 2007; Bureau of Transport and Regional Economics [BTRE], 2007).

Table 2

Statistics for aerosol data measured by FLAPS-III. Analysis of SS Total Count and FL/SS Count Ratios include all data ($N = 359,571$; total sampling time ~ 500 h) measured in 5 s; Results for FL1 and FL2 Total concentration were derived from FLAPS-III and APS paired data ($N = 99,999$).

Parameter measured	Mean	STD	Median	IQR
SS Total Count	4376	4754	2849	2684
FL1[2–31]/SS Count Ratio	0.053	0.054	0.039	0.031
FL2[2–31]/SS Count Ratio	0.072	0.071	0.051	0.044
FL1[2–31]/FL2[2–31] Count Ratio	0.788	0.537	0.745	0.087
FL1 Total Concentration ($\# \text{ cm}^{-3}$)	0.046	0.076	0.023	0.025
FL2 Total Concentration ($\# \text{ cm}^{-3}$)	0.062	0.108	0.030	0.033

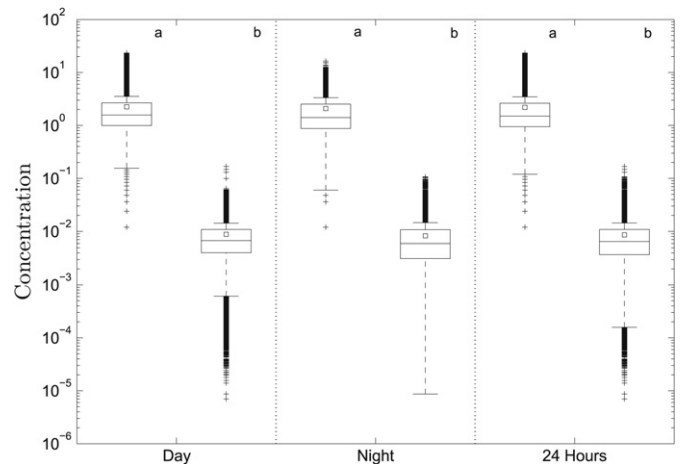


Fig. 1. Box plot of particle (a) number ($\# \text{ cm}^{-3}$) and (b) mass (mg m^{-3}) concentration measured by APS in the size range 1–10 μm during day (06:00–20:00, $n_{\text{Day}} \sim 153,906$); night (20:00–06:00, $n_{\text{Night}} \sim 91,468$); and 24 h, ($n_{24 \text{ h}} \sim 245,374$) periods. Mean value displayed as (\square); median (centre line); 25% and 75% bottom and top of rectangle respectively; whiskers set to $\pm 1.93\sigma$ for display purposes; outliers ($+$).

To evaluate further the daily variation in APS number and mass concentrations, all available data were grouped and averaged over 30 min time intervals. The averaged time series presented in Fig. 2 show a complex multi peak profile with two broad dominant modes (6:00–13:00) and (16:00–21:00) likely to be associated with an increased contribution from traffic during the traffic rush hours. In the morning, maximum number concentration was observed at about 09:00 ($\sim 2 \# \text{ cm}^{-3}$) while in the afternoon/evening mode the maximum was observed at about 20:00 ($\sim 1.7 \# \text{ cm}^{-3}$). There seems to be also relatively high concentration at night between 23:00 and 03:00, which could be associated with the emissions from local industrial sources operating 24/7 (e.g. dockside activities).

To investigate the trends further (in an attempt to unmask the effect of local emission sources), the daily averages of particle number and mass concentration were normalised by the night average (i.e. median night values of dN and dM, respectively).

Perhaps not surprisingly, the normalised concentrations show similar trends as observed in Fig. 2 with two dominant modes observed in the morning and late afternoon/evening. The concentration levels reached up to 1.4 times the night level between 09:00–11:00 and up to 1.2 times at around 20:00 (dN). Relatively

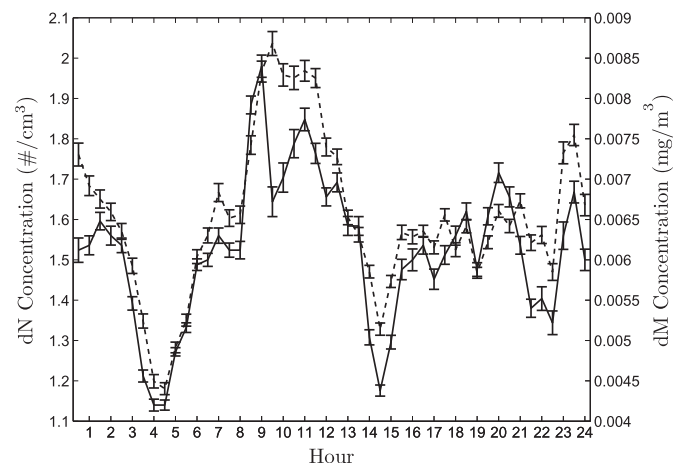


Fig. 2. 30 min average (Median \pm IQR/ \sqrt{n}) of number (dN, solid line) ($\# \text{ cm}^{-3}$) and mass (dM, dashed line) (mg m^{-3}) concentrations measured by APS in the size range 1–10 μm . (Number of data points $n = 245,374$; 5 s readings).

low concentrations were observed for 03:00–05:00 and 13:00–15:00 time periods. The fluctuations could be associated with changes in emission sources (mainly traffic density) contributing to the measured background and changes in atmospheric conditions driving the aerosol dispersion (wind, convection, etc.).

A similar trend as presented in Fig. 2 was reported in a study conducted in Brisbane by Mejía et al. (2007) for a comparable type of sampling environment (emission sources, location and topography). The authors showed a strong dependency of sub-micrometer particle concentration on traffic emissions (traffic density; type of cars) and wind direction. A review of the dependencies of ambient background on the meteorological conditions is presented for example in Harrison et al. (2004).

4.2. FLAPS-III data

The statistics for FLAPS-III data measured over a period of 500 h is presented in Table 2. The SS counts represent the total aerosol particles (TAPs) and FL counts the fluorescent biological particles (FBAPs) in the 1–10 μm size range measured over 5 s sampling intervals. FL1[2–31] and FL2[2–31] correspond to integrated particle count in bins [2–31] for the gated fluorescent light intensity as discussed previously.

The median values for FL1/SS and FL2/SS ratio were 3.9% (FL1) and 5.1% (FL2), respectively. The mean values were 5.3% (FL1) and 7.2% (FL2). Correlation analysis of fluorescence measurements (5 s readings) showed high correlation ($R^2 \sim 99\%$) indicating that fluorescence (from both FL1 and FL2 channels) originated from the same batch of processed particles. Natural fluorescence responses from UV light tend to have quite broad emission spectrums which may overlap the wavelength range of both PMTs. For instance, fluorescence emission from NAD(P)H will primarily be in the FL1 band but will also extend to FL2. The FLAPS-III optical design (excitation wavelength 405 nm; detection band for FL1 (430–500 nm); FL2 (500–600 nm)) and factory calibration assumes that the signal levels obtained from FL1 and FL2 channels can be treated as equal in magnitude. Based on that assumption our results indicate that in terms of particle number, the FBAPs represent about 4–5% (median) of TAPs.

The number of fluorescent particles in the FL2 channel was higher compared to FL1, with the FL1/FL2 count ratio 0.79 (mean) and 0.75 (median). This effect could be associated with differences in fluorescence originating from different molecules (e.g. NAD(P)H and riboflavin) and different organisms (Agranovski and Ristovski, 2005; Hill et al., 2009; Brosseau et al., 2000).

Correlation between the fluorescent (FL1; FL2) and total (SS) count rate was also high ($0.82 \leq R^2 \leq 0.84$), which indicates a relatively high association between the FL and SS data.

The presented results for total (SS count) and FBAPs are relative values; dependent on the physical properties of sampled material, size distribution of aerosols and FLAPS-III sampling characteristics. Using the absolute quantification of particle concentration capability of APS (TAPs), and the method described in Section 2.3, concentration estimates from FLAPS-III counts can be calculated. Although the instruments use different measuring techniques (APS: Time-of-flight, FLAPS-III: light scattering), a fairly acceptable correlation value of 69.3% between the instruments was achieved over the measuring period.

The measured fluorescent particle concentrations (mean values of 0.046 (FL1) and 0.062 (FL2) $\# \text{cm}^{-3}$) are in good agreement with the literature. Huffman et al. (2010) for comparison, reported the mean number concentration of FBAPs in the 1–10 μm size range of 0.03 $\# \text{cm}^{-3}$ – measured in a similar type of ambient environment.

Further exploration of the fluorescent concentration dependencies and behaviour was not the focus of this work and will be

presented in a follow up publication. Since the measured FLAPS-III data will be used in relative terms as a ratio of FL/SS or normalised SS count, the terms count and concentration will be used interchangeably throughout the following sections.

Similar to the APS data, the FL/SS ratios derived from FLAPS-III data were analysed for different time intervals (day, night and 24 h) as presented in Fig. 3. Several observations can be made from this data: the FL2/SS values were consistently higher compared to FL1/SS values for both (day and night) datasets; the fluorescent content was higher during the day compared to night ($(\text{FL/SS})_{\text{Day}} > (\text{FL/SS})_{\text{Night}}$) values showed a narrower spread (IQR) compared to night results and were shifted towards the lower values (smaller fraction of fluorescence). Analysis of the medians difference (Mann–Whitney two sample rank-sum test) showed statistically significant difference between the medians of FL1/SS and FL2/SS for day, night and 24 h time periods (at the 95% confidence level).

The daily variation in fluorescent particle loading calculated as 30 min averages is presented in Fig. 4. The fraction of fluorescent particles varied throughout the day between 3–7% (FL1/SS) and 4–9% (FL2/SS). The variation has diurnal character with the most dominant peaks appearing at around 11:00 and 15:00. The fluorescent particle content showed a steady increase starting at about 5:00 until 9:00, with a sharp increase peaking at 10:30. A second, less pronounced maximum can be observed at about 15:00.

To discern the dependencies and behaviour of the 24 h daily data, the daily variation of FL and SS data were normalised by the night values as presented in Fig. 5. It can be seen that the SS data shows several peaks throughout the day (the most dominant being between 10:00 and 12:00) while FL1 and FL2 signals exhibit two broad distinct modes (peaks). Similar to the SS data, the most dominant peaks for FL1 and FL2 are observed at about 10:00. The FL levels start to increase at about 05:00 which could be associated with the emission from biogenic sources linked to sunrise with a further steady increase between 08:00–09:00 and then a very rapid climax with a peak at 10:30. We speculate that the dominant mode during 10:00–12:00 period could be associated with the presence of biological material originating from different biogenic sources (e.g. marine environment) emerging as a result of changed environmental conditions (e.g. wind direction) and is consistent with the rhythm of anthropogenic activities in the surrounding urban area. Other factors influencing FL/SS fluctuations could be

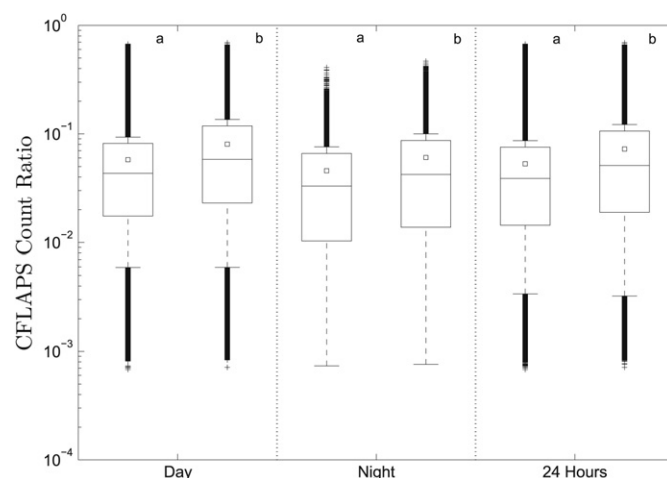


Fig. 3. Box plot of (a) FL1/SS and (b) FL2/SS count ratio measured by FLAPS-III in the size range 1–10 μm during day (06:00–20:00; $N_{\text{Day}} \sim 216,188$), night (20:00–06:00; $N_{\text{Night}} \sim 143,383$) and 24 h ($N_{24 \text{ h}} \sim 359,571$) periods. Mean value displayed as (\square); median (centre line); 25% and 75% bottom and top of rectangle respectively; whiskers set to $\pm 1.58\sigma$ for display purposes; outliers (+).

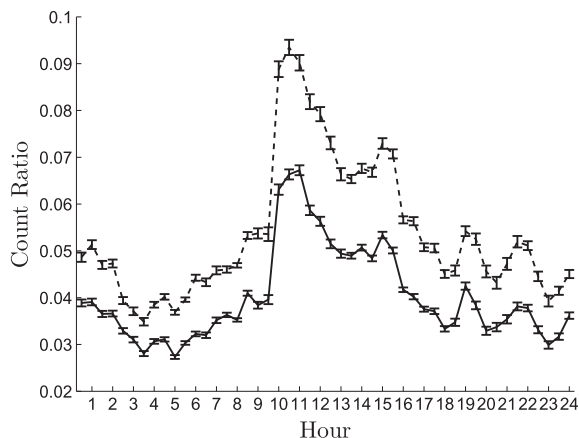


Fig. 4. FL1/SS (solid line) and FL2/SS (dashed line) Ratio's, 30 min median averages. (IQR/ \sqrt{n} shown as error bars).

attributed to different biological material composition with different strengths of fluorescence (Coz et al., 2010). Investigation of the composition of the biological materials and their source apportionment was beyond the scope of this study.

An indirect validation of our results was obtained through comparison with the results of other studies focused on biobackground characterisation using optical and biological methods as outlined below.

Boulet et al. (1996), based on a review of previous studies in different locations, showed that under normal, steady state background atmospheric conditions the fraction of fluorescent particles rarely exceeded 5%.

Monitoring of fluorescence in ambient air measured in Calgary CA, where relatively high levels of human and vegetative contributions could be expected, the fluorescent fraction of ambient aerosol in the 2.5–10 μm range rarely exceeded 5% regardless of the total particle number concentration (Ho and Spence, 1998).

Coz et al. (2010) reported that PBAPs measured in an urban area in the northeastern United States contributed to PM on average $6.9 \pm 5.4\%$ during summer and $3.3 \pm 1.4\%$ during winter. The high variability during summer could be attributed to short term variations in both the load and composition of bacterial aerosols. The small variability found during winter suggest the existence of a relatively constant background level of PM PBAPs mass of 2–5%.

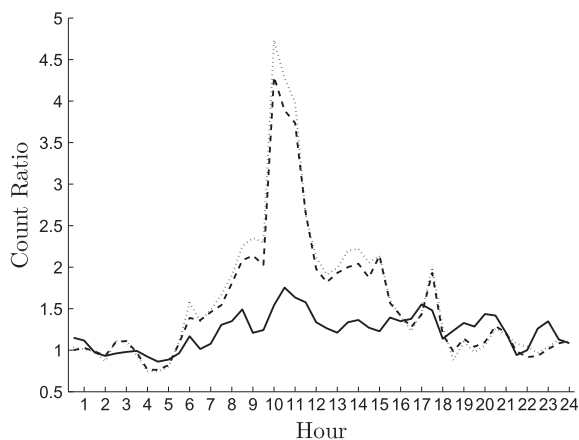


Fig. 5. 30 min averages (Median) for FLAPS-III particle count normalised by the median night count for total (SS [solid line]) and Fluorescent (FL1 [dashed line]) particles in the 1–10 μm size range. Median night values of 2430 for SS, 72 for FL1 and 91 for FL2. 359570 data points. 5 s samples.

In a study very similar to the presented work, Huffman et al. (2010) characterised the biobackground in Mainz, Germany in a semi-urban environment. Using similar experimental and sampling setups (FLAPS-III sampling from a building roof close to the CBD) over several months, the authors reported about 4% of FBAPs in terms of particle number and about 20% in terms of particle mass.

In summary, the measured data are in a good agreement with results reported in literature in terms of TAP and FBAPs concentration, fluorescent content (FL/SS) and their fluctuation during the day. These results imply validity of the collected data set and its suitability for further exploration using advanced statistical methods aiming to develop superior alarm trigger algorithms.

5. Model of biobackground

Particles in the biobackground are in continuous motion (with random displacements) and are being advected by turbulent flow in the atmospheric surface layer. Due to their size (1–10 μm) the inverse effect of these particles on flow is negligible and their kinematics can be described by the models of 'passive scalar' turbulence (or turbulent Lagrangian transport) Falkovich et al. (2001). This means that one can introduce the instantaneous concentration of the particles $\theta(\mathbf{r}, t)$ that obeys a stochastic equation of concentration transport (the stochasticity of the transport equation is a result of the randomness of the underlying turbulent velocity field). In other words, the theory of scalar turbulence provides a consistent framework for derivation of the statistical properties of concentration $\theta(\mathbf{r}, t)$ (i.e. moments, PDFs and correlations) for given statistics of velocity. Remarkably, some important properties of particle statistics experimentally observed in complex environmental settings (boundary layer flow, strong anisotropy, buoyancy etc.) emerge from the simplest (but still justifiable) models of turbulent flow i.e. white-noise or the Kraichnan model (Falkovich et al., 2001). From this perspective we anticipated that certain statistical characteristics of the biobackground should also reflect the fundamental properties of underlying mixing processes, irrespective of the nature (biological/non-biological) of the aerosol particles. This was the main rationale behind our approach to the exploration of our experimental data and the development of a statistical framework as outlined below.

One of the most interesting predictions of the theory of scalar turbulence applied to transport in the atmospheric surface layer is the conclusion that all statistical moments of the scalar concentration $\langle \theta^n(\mathbf{r}, t) \rangle$ are expected to follow the same profile, regardless of the value of n . This allows one to write the following simple scaling laws for the concentration moments (for details see Yee and Chan (1997); Lebedev and Turitsyn (2004); Yee (2009); Skvortsov and Yee (2011)).

$$\frac{\langle \theta^n \rangle}{\langle \theta \rangle^n} = \xi_n \left(\frac{\langle \theta^2 \rangle}{\langle \theta \rangle^2} \right)^{n-1}, \quad n \geq 2 \quad (1)$$

and

$$\langle \theta^2 \rangle \propto \langle \theta \rangle, \quad n = 2. \quad (2)$$

The pre-factor ξ_n in this expression has been theoretically evaluated for two extreme cases. For the case of a perfectly mixed tracer (which usually corresponds to locations far away from a tracer source) $\xi_n^- = 1$; while for the opposite, highly intermittent case (near the source region) $\xi_n^+ = \Gamma(n+1)/2^{n-1}$; where $\Gamma(\cdot)$ is the Gamma function (Skvortsov and Yee, 2011). Hence, in real situations we expect that particle concentration statistics should

follow the scaling law (1) with the pre-factor ξ_n located between these two estimates ($\xi_n^- \leq \xi_n \leq \xi_n^+$).

We found these predictions are in good agreement with our extensive observational data (see Figs. 6 and 7). The statistical moments of particle concentrations $\theta^n(\mathbf{r}, t)$ were calculated from time series recorded by the FLAPS-III (SS, FL1, FL2) and APS instruments at the same location, so $\theta(\mathbf{r}, t) \equiv \theta(t)$ in our case. The scaling laws (1) corresponding to the experimental data from FLAPS-III for $n = \{3, 4\}$ are depicted in Fig. 6 and compared with the theoretical predictions (1) and (2).

The non-biological contribution (top plot in Fig. 6) comes from the SS channel of FLAPS-III and the biological (bottom plot in Fig. 6) from the summation of the FL1 and FL2 channels. Since FL1 and FL2 are strongly correlated the aggregated FL1 + FL2 metric captures all relevant data and removes the need to analyse both channels separately. APS concentrations follow the same trends and are therefore not shown in the following analysis.

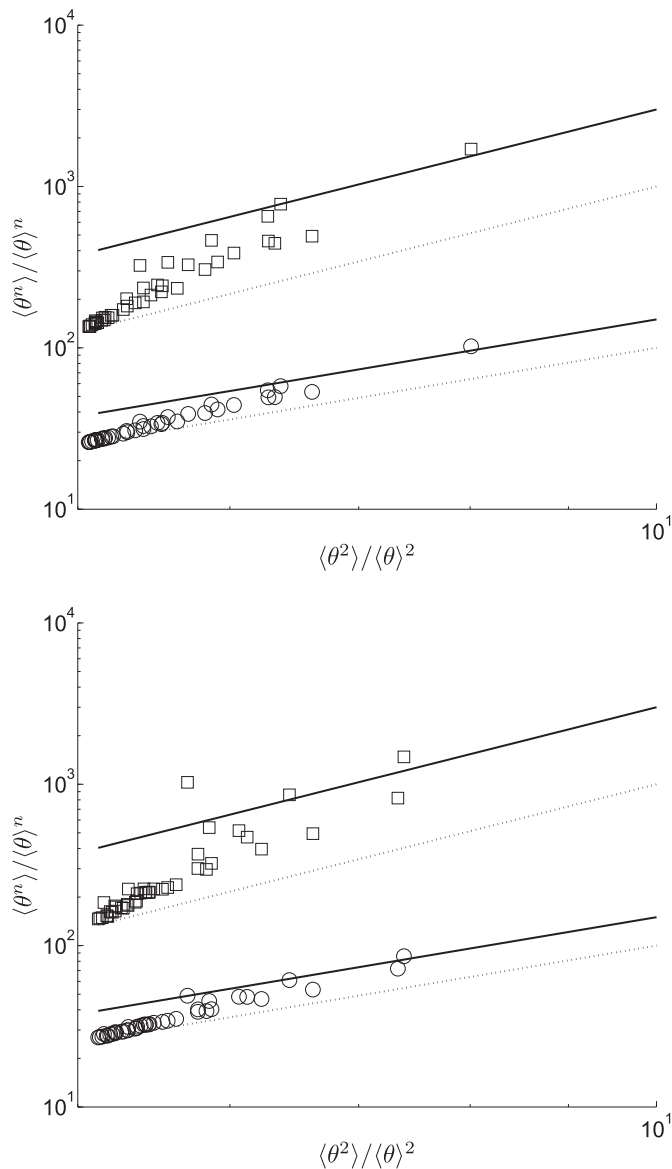


Fig. 6. Scaling laws for statistical moments of particle concentration. Top plot represents non-biological material (SS) and the bottom biological (FL1+FL2). Bottom and top data series on each plot correspond to moments $n = 3$ (\circ) and $n = 4$ (\square) respectively. Lines correspond to the theoretical relationship (1) with two different values of pre-factor $\xi_n = \xi_n^-$ (dashed line), $\xi_n = \xi_n^+$ (solid line), see text for details.

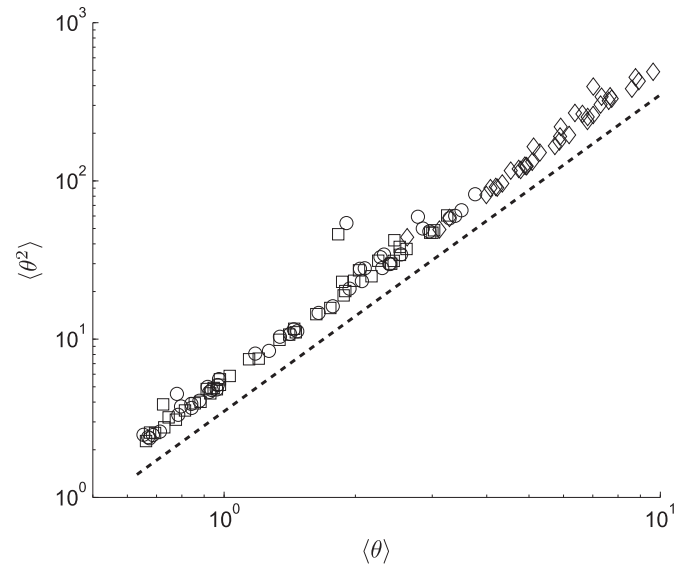


Fig. 7. Similarity of scaling laws for statistical moments of particle concentration for biological (FL1: \square , FL2: \circ) and non-biological (SS: \diamond) particles, see text for details. The dashed line corresponds to the theoretical prediction (2), with a scaling constant of 3.5 for visual appearance only.

The experimental data follows the scaling laws (1) reasonably well within a wide range of measured concentrations (see Fig. 3 and Table 2) with the pre-factor value ξ_n extensively occurring in the expected range $\xi_n^- \leq \xi_n \leq \xi_n^+$. For the $n = 2$ case (2), a similar plot is presented in Fig. 7. Since pre-factor ξ_2 is not defined in (2), a value of 3.5 was assigned for better visual appearance on the theoretical fit. From Fig. 6, we can see that when applied to the biobackground the scaling laws (1), (2) become less accurate for higher order moments (i.e. higher n) from the presence of outliers above the ξ_4^+ bound on the bottom plot of Fig. 6. This is similar to the case of tracer dispersion from localised sources (Yee and Skvortsov, 2011). Nevertheless, with the two theoretical values of pre-factor they always provide a valuable tool for the estimation of the statistical moments of the aerosol particle concentration in the atmospheric surface layer.

To validate our scaling conjecture further and to prove its independency of the particles' origin we present the scaling law (2) of biological and non-biological sources in Fig. 7. We observe that the scaling law (2) of the statistical moments of the biobackground concentration are in excellent agreement with the prediction of the scalar turbulence theory, i.e. they are mostly determined by the kinematics of the turbulent surface layer.

It is worth stressing that the scaling laws (1) and (2) manifest a general property of turbulent mixing and are not a consequence of any particular functional form of concentration PDF $p(\theta)$. Contrarily, any distinct PDF form should comply with these scaling laws and this compliance is one of the important criterion for the evaluation of appropriate candidate model for $p(\theta)$.

Amongst the different functional PDF forms of tracer concentration evaluated in studies of turbulent tracer dispersion, the Gamma form has recently emerged as one that adequately captures the physics of turbulent transport and provides a good match with a variety of experimental data (Yee and Chan, 1997; Skvortsov and Yee, 2011). This model (see the Gamma form of (3)) can be analytically derived using a phenomenological analogy between the mixing and convection processes by explicit modelling of the deformation of tracer blobs by random stretching and folding (Duplat and Villermaux, 2008; Villermaux and Duplat, 2003; Venaille and Sommeria, 2008). Indeed, the Gamma PDF complies

with the scaling laws of the concentration moments (1), (2) with the pre-factor ξ_n residing within the range $\xi_n^- \leq \xi_n \leq \xi_n^+$ described above (for details see Yee and Skvortsov (2011)). Whilst the Gamma distribution is defined with two parameters (scale θ and shape k), it can also be written in a “single-parameter” form (Yee and Chan, 1997; Yee, 2009; Duplat and Villiermaux, 2008; Villiermaux and Duplat, 2003):

$$p(\chi \equiv \theta / \langle \theta \rangle) = \frac{k^k}{\Gamma(k)} \chi^{k-1} \exp(-k\chi), \quad (3)$$

where k is the only fitting parameter of the model and can be related to the statistical moments by (Yee and Skvortsov, 2011)

$$\frac{1}{k} = \frac{\langle \theta^2 \rangle}{\langle \theta \rangle^2} - 1. \quad (4)$$

From these two equations we can see that our model of the bio-background is uniquely determined by the first two moments (i.e. $\langle \theta \rangle$ and $\langle \theta^2 \rangle$), which is a well-known property of the Gamma distribution.

To verify the Gamma PDF model agrees with our experimental data, we compare it with the statistical properties of our observations (i.e. time series of particle concentrations from FLAPS-III). In order to do this; $\langle \theta \rangle$ is calculated for the bio- and non bio-particles, then histograms of our time series of concentration in terms of $\chi \equiv \theta / \langle \theta \rangle$ were produced. These histograms (or empirical Cumulative Distribution Functions (CDFs)) are compared with the CDF corresponding to the functional form of (3). In such an approach, k was the only parameter to fit from observations.

The results of this comparison are depicted in Fig. 8 (non-biological particles top; biological bottom). The tight fit shows that this model can be reliably used for the parametrisation of the statistical properties of ambient air (both biological and non-biological contributions). The estimations of parameter k were quite stable leading to values $k = 1.1$ for non-biological and $k = 1.8$ for biological particles. For non-biological particles the (mathematically) simpler Exponential PDF (i.e. (3) with $k = 1$) can be used as an approximate model for our data. This distribution has a k value of 1.1 and therefore a relatively small deviation of 0.1 from the $k = 1$ required for the Exponential form. The significant advantage of the Exponential model (even taking into account its inferior data fit compared to Gamma, see both plots on Fig. 8) is that it requires fewer parameters to estimate and to fit. For instance; the Exponential PDF model can be used for rapid calibration of a detection system when only a limited set of data for the monitored environment has been collected. The biological contribution (bottom plot of Fig. 8) is described quite poorly by the Exponential PDF. This contribution (the presence of biological material) can therefore be easily identified just by monitoring the value of k . Investigation of this dependency will be the first parameter of interest in our future publication on biodetection algorithms.

The Gamma model (3) does not take into account the intermittency of a particle distribution (i.e. a finite probability that the particle concentration is exactly zero for a certain period of time). This model is therefore only valid for perfectly mixing tracer flows – which rarely occur naturally. In order to estimate the effect of intermittency we appropriately modified our concentration PDFs by adding an intermittency correction (for details see Yee and Chan, 1997; Yee, 2009; Skvortsov and Yee, 2011 and references therein)

$$p(\theta) = (1 - \gamma)\delta(\theta) + \gamma\tilde{p}(\theta), \quad (5)$$

where $\delta(\cdot)$ is the delta function, γ is the intermittency factor (a degree of mixing with $\gamma = 1$ corresponding to the perfect mixing case), $\tilde{p}(\theta)$ is the “regular” PDF (in our case (3)). The estimation of

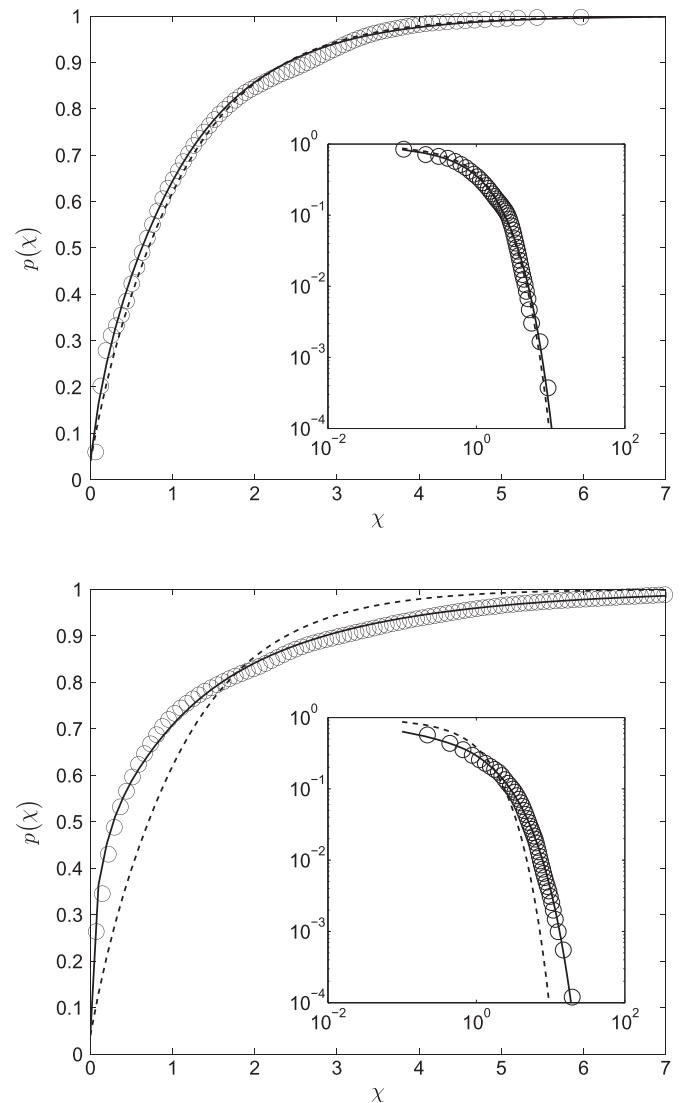


Fig. 8. CDFs of non-biological (SS, top plot) and biological (FL1+FL2, bottom plot) particle concentrations (\circ) with intermittency correction (5). Gamma (solid line) and Exponential (dashed line) models are also shown. Inserts show the Exceedance Distribution Function (1-CDF) of the same data and models, see text for details.

parameter γ in the model (5) from concentration time series is well established in the studies of turbulent dispersion (Yee and Chan, 1997; Yee, 2009; Skvortsov and Yee, 2011 and references therein), so we omit all technical details and present only the main results. We found that the effect of γ is not significant in our data, i.e. γ was always close to unity. A stable estimation from both FLAPS-III and APS yield a consistent value $\gamma \approx 0.97$, which is exemplified in the small positive shift in the $p(\chi)$ -intercept from 0 in Fig. 8. Nevertheless, since the value of γ is also determined by the proximity to a particle's source, we expect that in some cases the intermittency correction in the model (5) may become appreciable (Yee and Chan, 1997; Yee, 2009).

If this is the case, γ will be the second parameter of interest in our biodetection algorithm. This assumption also leads to two important conclusions. Firstly, there should be a significant similarity between bio- and non bio-aerosol characteristics measured at the same location (since they undergo the same mixing process). Secondly, these characteristics should clearly comply with the physics of turbulent mixing. As illustrative examples we mention here a universal relationship between statistical moments of

particle concentration (a so-called scaling law) and the explicit functional form for the probability distribution function of particle concentration (the Gamma function). It is worth remarking in this context, that the scaling law for statistical moments is more general and is not bound to a particular functional form of concentration PDF (Lebedev and Turitsyn, 2004).

6. Conclusions and future work

In summary, we quantified the content of ambient background for an urban/industrial type of environment close to the Melbourne CBD. Concentration of total and biological aerosols in the 1–10 μm size range was monitored over several days and the results of exploratory analyses for day, night and daily (24 h) fluctuations are presented.

The measures of total particle *number* and *mass* concentration are in good agreement with previous results obtained for the Melbourne area. Daily profiles (30 min averages) shows complex behaviour with two dominant modes observed in the morning and afternoon/evening corresponding to traffic peaks hours. The results indicate that the ambient background loading is dominated by vehicular traffic emissions.

The fraction of fluorescent particles in total was in the range of 3–9% (30 min average) which is in good agreement with other studies reported in the literature. Concentration levels of biological material showed diurnal variation which could be associated with an increase in emissions and changes of biogenic sources. The levels increased up to four times during the midday period as compared to the night mean values. Our results are in good agreement with the study Huffman et al. (2010); conducted in a similar type of ambient environment.

A universal model of the biobackground has been produced from this data set that provides a rigorous framework for the development of novel algorithms for bio-aerosol detection/characterisation and can help to both improve and optimise some existing algorithms used in operational systems.

These refinements may be implemented by initially using the scaling laws (1) and (2), which provide an efficient way to estimate any statistical moment from a limited data set. For instance, moments can be obtained even if only a few concentration levels are known (measured) or measurements are of poor quality. This implies that by employing relationship (1) we can continuously infer the mixing state of the biobackground, i.e. how close its distribution is to the equilibrium state. In effect, any deviation from the equilibrium scaling given by law (1) would indicate the proximity of a bio-aerosol release. This important capability (i.e. estimation of proximity to the biological source) is the main strength and novelty of the proposed model and can be used for the development of new, robust biodetection algorithms. Secondly, the specific PDF form the biobackground (i.e. Gamma PDF) enables a rigorous assignment of a well-defined measure (based on likelihood or risk) that is associated with any detected spike in bio-aerosol measurement. An informative decision regarding the relevance of this spike can then be made according to the current operational context (e.g. it may provide a consistent methodology to reduce the false alarm rate), resulting in rigorous risk mitigating strategies. Lastly, the deep analogy between bio- and non-bio particle distributions emerging from the physics of turbulent mixing allows significant simplification of any calibration process for deployable systems (including the capability for rapid self-calibration), by extracting additional statistical information from monitoring the non-biological aerosol background.

A monitoring system such as this would enable conscious operational decisions to be employed which can help to develop more robust instrumentation algorithms for the detection of

biothreats in operational settings, rigorously evaluate the risk associated with miss and false detection as well as to propose relevant mitigation strategies in response to the detected bio-release. Specifics concerning this framework will be elaborated upon in future publications.

Acknowledgements

This work was supported by DSTO Task 07/086 (Civilian Counter Terrorism and National Security–Public Safety Program) and DSTO Task 07/301 (BioCERP, Bio-surveillance).

The authors would like to acknowledge assistance and support received from Dinesh Pitaliadda, Mark Ryan, Andrew Walker, Gerry Parkinson, Wendy Muir and other colleagues from DSTO who contributed to the project. We thank Chris Woodruff (DSTO) for his careful reading of the manuscript; Jim Ho (DRDC Suffield, CA) and Chris Bliss, (Dycor Technologies) for their assistance in regards to FLAPS technology.

References

- Agranovski, V., Ristovski, Z., Hargreaves, M., Blackall, P.J., Morawska, L., 2003a. Performance evaluation of the UVAPS: influence of physiological age of airborne bacteria and bacterial stress. *Journal of Aerosol Science* 34, 1711–1727.
- Agranovski, V., Ristovski, Z., Hargreaves, M., Blackall, P.J., Morawska, L., 2003b. Real-time measurement of bacterial aerosols with the UVAPS: performance evaluation. *Journal of Aerosol Science* 34, 301–317.
- Agranovski, V., Ristovski, Z.D., 2005. Real-time monitoring of viable bioaerosols: capability of the UVAPS to predict the amount of individual microorganisms in aerosol particles. *Journal of Aerosol Science* 36, 665–676.
- Agranovski, V., Ristovski, Z.D., Ayokoa, G.A., Morawska, L., 2004. Performance evaluation of the UVAPS in measuring biological aerosols: fluorescence spectra from NAD(P)H coenzymes and riboflavin. *Aerosol Science and Technology* 38, 354–364.
- Ariya, P.A., Sun, J., Eltouny, N.A., Hudson, E.D., Hayes, C.T., Kos, G., 2009. Physical and chemical characterization of bioaerosols – implications for nucleation processes. *International Reviews in Physical Chemistry* 28, 1–32.
- Baron, P.A., Willeke, K., 2005. *Aerosol Measurement – Principles, Techniques, and Applications*, second ed. John Wiley & Sons.
- Bauer, H., Schueller, E., Weinke, G., Berger, A., Hitznerberger, R., Marr, I.L., Puxbaum, H., 2008. Significant contributions of fungal spores to the organic carbon and to the aerosol mass balance of the urban atmospheric aerosol. *Atmospheric Environment* 42, 5542–5549.
- Boulet, C.A., Ho, J., Stadnyk, L., Thompson, H.G., Spence, M.R., Luoma, G.A., Elaine, R.E., Lee, W.E., 1996. Memorandum no. SR 652 (unclassified). Technical Report. Defence Research Establishment Suffield. Canadian Defense Documents available at Information Holdings–Operations Department of National Defence, Ottawa, Ont., Canada.
- Brosseau, L.M., Vesley, D., Rice, N., Goodell, K., Nellis, M., Hairston, P., 2000. Differences in detected fluorescence among several bacterial species measured with a direct-reading particle sizer and fluorescence detector. *Aerosol Science and Technology* 32, 545–556.
- Bureau of Transport and Regional Economics [BTRE], 2007. Estimating Urban Traffic and Congestion Cost Trends for Australian Cities, Working Paper 71. Technical Report. BTRE, Canberra ACT.
- Burrows, S.M., Elbert, W., Lawrence, M.G., Pöschl, U., 2009. Bacteria in the global atmosphere – Part 1: Review and synthesis of literature data for different ecosystems. *Atmospheric Chemistry and Physics* 9, 9263–9280.
- Buteau, S., Simard, J.R., Rowsell, S., Roy, G., 2010. Bioaerosol standoff detection and correlation assessment with concentration and viability point sensors. *Proceeding of the SPIE* 7838, 78380J.
- Coz, E., Artífano, B., Clark, L.M., Hernandez, M., Robinson, A.L., Casuccio, G.S., Lersch, T.L., Pandis, S.N., 2010. Characterization of fine primary biogenic organic aerosol in an urban area in the northeastern United States. *Atmospheric Environment* 44, 3952–3962.
- Duplat, J., Villermaux, E., 2008. Mixing by random stirring in confined mixtures. *Journal of Fluid Mechanics* 617, 51–86.
- Dycor, 2011a. CFLAPS: Fluorescent Aerosol Particle System. <http://www.dycor.com/Products/DefenseSecurity/CBRNESurveillanceSolutions/CFLAPS.aspx> (accessed 11.08.11.).
- Dycor, 2011b. CFLAPS Specifications Sheet. <http://www.dycor.com/Portals/39/pdf/dycor/cflaps/feb2011.pdf> (accessed 11.08.11.).
- Eng, J., Lynch, R., Balaban, R., 1989. Nicotinamide adenine dinucleotide fluorescence spectroscopy and imaging of isolated cardiac myocytes. *Biophysical Journal* 55, 621–630.
- Environmental Protection Agency, 2009. Victoria's Air Quality 2009, Air Monitoring Data. <http://www.epa.vic.gov.au/Air/monitoring/air-monitoring-report-2009.asp> (accessed 17.03.11.).

- Falkovich, G., Gawedzki, K., Vergassola, M., 2001. Particles and fields in fluid turbulence. *Reviews of the Modern Physics* 73, 913–975.
- Gabey, A.M., Gallagher, M.W., Whitehead, J., Dorsey, J., 2009. Measurements of coarse mode and primary biological aerosol transmission through a tropical forest canopy using a dual-channel fluorescence aerosol spectrometer. *Atmospheric Chemistry and Physics Discussions* 9, 18965–18984.
- Hairston, P.P., Ho, J., Quant, F.R., 1997. Design of an instrument for real-time detection of bioaerosols using simultaneous measurement of particle aerodynamic size and intrinsic fluorescence. *Journal of Aerosol Science* 28, 471–482.
- Harrison, R.M., Jones, A.M., Lawrence, R.G., 2004. Major component composition of PM₁₀ and PM_{2.5} from roadside and urban background sites. *Atmospheric Environment* 38, 4531–4538.
- Hill, S.C., Mayo, M.W., Chang, R.K., 2009. Fluorescence of Bacteria, Pollens, and Naturally Occurring Airborne Particles: Excitation/Emission Spectra. Technical Report ARL-TR-4722. U.S. Army Research Laboratory.
- Hill, S.C., Pinnick, R.G., Niles, S., Pan, Y.L., Holler, S., Chang, R.K., Bottiger, J., Chen, B.T., Orr, C.S., Feather, G., 1999. Real-time measurement of fluorescence spectra from single airborne biological particles. *Field Analytical Chemistry and Technology* 3, 221–239.
- Ho, J., Duncan, S., 2005. Estimating aerosol hazards from an Anthrax letter. *Journal of Aerosol Science* 36, 701–719.
- Ho, J., Spence, M., 1998. Background aerosol characteristics measured with a fluorescence aerodynamic particle sizer: sensitivity of FLAPS performance. Defence Research Establishment Suffield 1504, 1–20.
- Ho, J., Spence, M., Hairston, P., 1999. Measurement of biological aerosol with a fluorescent aerodynamic particle sizer (FLAPS): correlation of optical data with biological data. *Aerobiologia* 15, 281–291.
- Huffman, J.A., Treutlein, B., Pöschl, U., 2010. Fluorescent biological aerosol particle concentrations and size distributions measured with an Ultraviolet Aerodynamic Particle Sizer (UV-APS) in Central Europe. *Atmospheric Chemistry and Physics* 10, 3215–3233.
- Jaenicke, R., Matthias-Maser, S., Gruber, S., 2007. Omnipresence of biological material in the atmosphere. *Environmental Chemistry* 4, 217–220.
- Jamriska, M., Morawska, L., Mergersen, K., 2008. The effect of temperature and humidity on size segregated traffic exhaust particle emissions. *Atmospheric Environment* 42, 2369–2382.
- Jensen, J.G., 2007. Effect of Atmospheric Background Aerosols on Biological Agent Detectors. Technical Report. Headquarters U.S. Air Force.
- Kanaani, H., Hargreaves, M., Smith, J., Ristovski, Z., Agranovski, V., Morawska, L., 2008. Performance of UVAPS with respect to detection of airborne fungi. *Journal of Aerosol Science* 39, 175–189.
- Keywood, M.D., Ayers, G.P., Gras, J.L., Gillett, R.W., Cohen, D.D., 1999. Relationships between size segregated mass concentration data and ultrafine particle number concentrations in urban areas. *Atmospheric Environment* 33, 2907–2913.
- Lafamme, C., Verreault, D., Lavigne, S., Trudel, L., Ho, J., Duchaine, C., 2005. Auto-fluorescence as a viability marker for detection of bacterial spores. *Frontiers in Bioscience* 10, 1647–1653.
- Lebedev, V., Turitsyn, K., 2004. Passive scalar evolution in peripheral regions. *Physical Review E* 69, 036301.
- Mejía, J., Wraith, D., Mengersen, K., Morawska, L., 2007. Trends in size classified particle number concentration in subtropical Brisbane, Australia, based on a 5 year study. *Atmospheric Environment* 41, 1064–1079.
- Morawska, L., Johnson, G., Ristovski, Z.D., Agranovski, V., 1999. Relation between particle mass and number for submicrometer airborne particles. *Atmospheric Environment* 33, 1983–1990.
- Peters, T.M., Leith, D., 2003. Concentration measurement and counting efficiency of the aerodynamic particle sizer 3321. *Journal of Aerosol Science* 34, 627–634.
- Pinnick, R.G., Hill, S., Pan, Y., 2009. Interactive comment on “Measurements of coarse mode and primary biological aerosol transmission through a tropical forest canopy using a dual-channel fluorescence aerosol spectrometer” by A. M. Gabey et al. *Atmospheric Chemistry and Physics Discussions* 9, C6744–C6751.
- Pinnick, R.G., Hill, S.C., Nachman, P., Videen, G., Chen, G., Chang, R.K., 1998. Aerosol fluorescence spectrum analyzer for rapid measurement of single micrometer-sized airborne biological particles. *Aerosol Science and Technology* 28, 95–104.
- Pitz, M., Cyrus, J., Karg, E., Wiedensohler, A., Wichmann, H.E., Heinrich, J., 2003. Variability of apparent particle density of an urban aerosol. *Environmental Science & Technology* 37, 4336–4342.
- Pöschl, U., 2005. Atmospheric Aerosols: composition, transformation, climate and health effects. *Angewandte Chemie International Edition* 44, 7520–7540.
- Semler, D.D., Roth, A.P., Semler, K.A., Nolan, P.M., 2004. Simulated field trials using an indoor aerosol test chamber. In: Scientific Conference on Chemical and Biological Defense Research. Dycor Technologies Ltd., Edmonton, Canada.
- Setlow, B., Setlow, P., 1977. Levels of acetyl coenzyme A, reduced and oxidized coenzyme A, and coenzyme A in disulfide linkage to protein in dormant and germinated spores and growing and sporulating cells of bacillus megaterium. *Journal of Bacteriology* 132, 444–452.
- Sivaprakasam, V., Huston, A., Scotto, C., Eversole, J., 2004. Multiple UV wavelength excitation and fluorescence of bioaerosols. *Optics Express* 12, 4457–4466.
- Skvortsov, A., Jamriska, M., DuBois, T.C., 2010. Scaling laws of passive tracer dispersion in the turbulent surface layer. *Physical Review E* 82, 056304.
- Skvortsov, A., Yee, E., 2011. Scaling laws of peripheral mixing of passive scalar in a wall-shear layer. *Physical Review E* 83, 036303.
- TRW Systems and Information Technology Group, 2001. A Primer on Biological Detection Technologies. Technical Report. North American Technology and Industrial Base Organization.
- Tsai, C.J., Chen, S.C., Huang, C.H., Chen, D.R., 2004. A universal calibration curve for the TSI aerodynamic particle sizer. *Aerosol Science and Technology* 38, 467–474.
- TSI, 2011. APS Specifications Sheet. <http://www.tsi.com/uploadedFiles/Product/Information/Literature/Spec/Sheets/3321.pdf> (accessed 11.08.11.).
- Venaille, A., Sommeria, J., 2008. Is turbulent mixing a self-convolution process? *Physical Review Letter* 100, 234506.
- Villermaux, E., Duplat, J., 2003. Mixing as an aggregation process. *Physical Review Letter* 91, 184501.
- Yee, E., 2009. Probability law of concentration in plumes dispersing in an urban area. *Environmental Fluid Mechanics* 9, 389–407.
- Yee, E., Chan, R., 1997. A simple model for the probability density function of concentration fluctuations in atmospheric plumes. *Atmospheric Environment* 31, 991–1002.
- Yee, E., Skvortsov, A., 2011. Scalar fluctuations from a point source in a turbulent boundary layer. *Physical Review E* 84, 036306.